Materials Research Bulletin 66 (2015) 226–230

Contents lists available at ScienceDirect

Materials Research Bulletin

journal homepage: www.elsevier.com/locate/matresbu

Effects of molybdenum doping and thermal annealing on the physical properties of amorphous In–Zn–O films

Shiu-Jen Liu [a,*], Kuei-Ching Wu [a], Kun-Cheng Peng [b]

[a] Department of Mathematics and Science (Pre-college), National Taiwan Normal University, Linkou District, New Taipei City 244, Taiwan
[b] Department of Materials Engineering, Mingchi University of Technology, Taishan District, New Taipei City 243, Taiwan

ARTICLE INFO

Article history:
Received 8 October 2013
Received in revised form 10 February 2015
Accepted 14 February 2015
Available online 19 February 2015

Keywords:
A. Amorphous materials
B. Sputtering
D. Magnetic properties
D. Optical properties
D. Electrical properties

ABSTRACT

Amorphous In–Zn–O (a-IZO) films doped with Mo were prepared on glass substrates by using magnetron co-sputtering technique. The Mo concentration was controlled by varying the sputtering power applied on the Mo target. The effects of Mo doping and thermal annealing on the electrical, optical and magnetic properties of the a-IZO films were studied. The electrical properties of a-IZO films were found to be strongly affected by Mo doping and thermal annealing. The optical transmission near the absorption edge of a-IZO films is enhanced by Mo doping due to the decrease in reflection. The optical bandgap estimated to be 3.2 eV of a-IZO films is unaffected by Mo doping and thermal annealing. Moreover, some of Mo-doped films exhibit room-temperature ferromagnetism after annealing.

1. Introduction

Transparent conducting oxide (TCO) films including In_2O_3, ZnO and SnO_2 have been extensively studied for optoelectronic device applications, such as transparent electrodes for flat panel displays and solar cells, transparent thin film transistors and light emitting diodes [1–3]. For being used as transparent electrodes, high transparency in the visible range (≥80%) and low resistivity ($\leq 5 \times 10^{-4}\ \Omega$-cm) are the essential requirements for these TCO films. Impurity doping is generally adopted to increase the carrier density and, therefore, enhance the conductivity of TCO films. For example, high electrical conductivity can be achieved by Sn^{4+} ions substituted into the In^{3+} sites in In_2O_3, i.e. Sn-doped In_2O_3 films (ITO). It was found that, for In_2O_3 films, the Mo doping drastically enhances the carrier mobility with more than twice the value of ITO films [4,5] but not degrades their optical transmission. First-principle band structure calculations on Mo-doped In_2O_3 suggest that magnetic exchange interactions splitting the Mo *d* states result in the smaller effective mass of carriers and hence larger mobility compared to ITO [6].

We previously found that the Mo doping in amorphous In–Ga–Zn–O (a-IGZO) films enhances the carrier mobility and induces room-temperature ferromagnetism (RTFM). Moreover, the correlation between the carrier mobility and RTFM in Mo-doped a-IGZO films implies a role played by the free electrons in the ferromagnetic interactions. Since both carrier density and mobility of a-IZO films are generally higher than those of a-IGZO films, we were motivated to fabricate Mo-doped a-IZO films and study the effects of Mo doping and thermal annealing on the physical properties of a-IZO films.

2. Experimental

Mo-doped and undoped a-IZO films used in this study were fabricated on glass substrates (Corning #1737) at 150 °C by using magnetron co-sputtering technique. The sputtering was conducted with a 75 W RF power applied on a In–Zn–O target with composition of In:Zn=1:1 at.% and DC power of 0, 2, 4, 6 and 8 W applied on a metallic Mo target to control the Mo concentration doped in the films. The distance between the target and substrates was 10 cm. The base pressure of the sputtering chamber was 1.0×10^{-6} Torr and the working pressure was maintained at 2.0×10^{-2} Torr with flowing argon (12.5 sccm). After a 20-min sputtering, the films were cooled down to room temperature. Oxygen vacancies were expected in the undoped and Mo-doped a-IZO films grown with no oxygen ambient pressure. The thickness of the films was about 50 nm determined by cross-section SEM images.

The content ratios of the chemical composition of films listed in Table 1 were estimated by using energy dispersive X-ray

* Corresponding author. Tel.: +886 277148400.
E-mail address: sjliu@ntnu.edu.tw (S.-J. Liu).

http://dx.doi.org/10.1016/j.materresbull.2015.02.039
0025-5408/

Table 1
P_{Mo} is the DC power applied on the Mo target during sputtering. In, Zn, and Mo are the content ratios of the chemical composition in the films. The Sample #1 is an undoped a-IZO film.

Sample no.	P_{Mo} (W)	In (at.%)	Zn (at.%)	Mo (at.%)
#1	0	45.8	54.2	0
#2	2	43.4	55.6	1.0
#3	4	44.8	51.6	3.6
#4	6	44.7	49.7	5.6
#5	8	43.7	48.8	7.5

spectrometry (EDS). Even though the content ratio [In]/[Zn] of the target is 1/1 (at.%), the content of In in the sputtered films is less than that of Zn. The [In]/[Zn] ratio of the films ranges from 0.78 to 0.9 at.%. And the Mo content ratio [Mo]/[In + Zn + Mo] (0, 1.0, 3.6, 5.6 and 7.5 at.%) increases with increasing the DC power applied on the Mo target.

The crystal structure of the films was examined by X-ray diffraction (XRD) patterns by using the Cu-Kα line (PANalytical X'Pert PRO MPD) in Bragg–Brentano geometry ($\theta/2\theta$ coupled). The data were collected from 2θ = 20–80° at a scan rate of 1° per minute. The 2θ step was 0.05°.

The valence state of Mo ions was investigated by X-ray photoelectron spectroscopy (XPS) analysis using the Thermo VG Scientific ESCALAB 250 system with a Al Kα X-ray source (1486.6 eV). The analysis chamber is equipped with a flood gun used for charge compensation when necessary. The XPS spectra are referenced to the C 1*s* photoemission line of 284.8 eV.

The Hall effect measurement and van der Pauw method were employed to obtain the electrical properties including resistivity (ρ), carrier density (n) and carrier mobility (μ). The optical transmission and reflection spectra of the films were recorded by using an UV-Vis spectrophotometer. The magnetization measurements were performed at room temperature on a Quantum Design SQUID magnetometer with fields applied parallel to the plane of the films.

To explore the effects of annealing, the films were thermally treated at 150 °C in air for 20 min and the measurements described above were carried out again.

3. Results and discussion

There is no sharp peak observed in the XRD scans, shown in Fig. 1, which reveals the amorphous structure of all films. Moreover, the amorphous structure of the films was not affected by the annealing treatment since the annealing temperature was the same as the growth temperature (150 °C) and the annealing time was only 20 min. The main effect of being annealed in air on the films is believed to be the reduction of the oxygen vacancies resulted from the growth of the films by sputtering in an argon flow mixed with no oxygen.

To characterize the valence states of the Mo ions in the as-grown films, XPS measurements on the Mo 3*d* were carried out and illustrated in Fig. 2(a). There is no peak observed for the undoped a-IZO film, Sample #1. Two peaks are inspected for Samples #2 and #3 and three peaks are inspected for Samples #4 and #5. These peaks are labeled as P1, P2, and P3 according to their positions. The exact values of the binding energy of these Mo 3*d* peaks are listed in Table 2. As seen in Table 2, the P1 peaks can be assigned to Mo^{6+} $3d_{3/2}$ [7]. The P2 peaks could be a combination of Mo^{6+} $3d_{5/2}$ and Mo^{4+} $3d_{3/2}$ [8]. The P3 peaks are contributed by Mo^{4+} $3d_{5/2}$. From the data listed in Table 2, the valence of Mo ions doped in Samples #2 and #3 is 6+, and the valences of Mo ions doped in Samples #4 and #5 are 6+ and 4+. The Mo 3*d* XPS of the annealed films are shown in Fig. 2(b). The valence of Mo ions in the annealed Samples

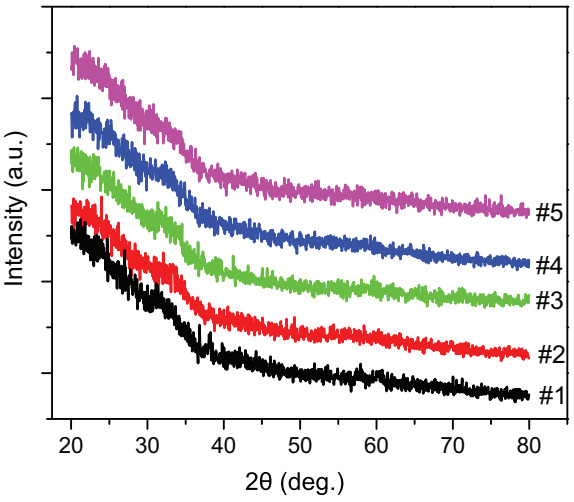

Fig. 1. X-ray diffraction scans of the Mo-doped and undoped a-IZO films. No sharp peak observed indicates the amorphous structure of films.

#2 and #3 is 6+, which is not affected by the annealing treatment. However, the P2 peaks of Samples #4 and #5 shift from 233.0 eV to 232.8 eV and from 233.2 eV to 232.9 eV, respectively. Since the binding energy of Mo^{6+} $3d_{5/2}$ is lower than that of Mo^{4+} $3d_{3/2}$, the shifts of the P2 peaks toward lower energy indicates the increase of the Mo^{6+} content in the annealed Samples #4 and #5, which is believed to be resulted from the reduction of the oxygen vacancies in the annealed films.

The optical transmission and reflection spectra of the as-grown films are illustrated in Fig. 3. The average transmission in the range of visible light of all films is about 80%. The transmission is obviously enhanced near the absorption edge, but it is slightly reduced in the range of wavelength longer than 430 nm by Mo doping. The effects of Mo doping on the transmission can be attributed to the variation of reflection. As seen in the figure, the reflection increases with increasing Mo doping below 430 nm and slightly decreases with Mo doping above 430 nm. The absorption coefficients (α) of the films are not affected by Mo doping. The optical bandgaps (E_g) of TCO films can be estimated by the relationship between α and photon energy ($h\nu$) of the form $(\alpha h\nu) \sim (h\nu - E_g)^r$ with $r = 2$ suggested by Tauc for amorphous semiconductors [9,10]. Since the absorption of films is not affected by annealing and Mo doping, the E_g of all films is nearly the same

Table 2
The positions of the Mo 3*d* peaks observed in the XPS spectra.

Sample no.	P1 (eV)	P2 (eV)	P3 (eV)
As-grown			
#2	236.0	232.8	–
#3	236.0	232.7	–
#4	235.8	233.0	230.6
#5	235.9	233.2	230.4
Annealed			
#2	236.0	232.8	–
#3	235.9	232.7	–
#4	235.6	232.8	230.6
#5	235.4	232.9	230.4
Mo^{6+} $3d_{3/2}$ [a]	235.8		
Mo^{6+} $3d_{5/2}$ [a]		232.6	
Mo^{4+} $3d_{3/2}$ [b]		233.2	
Mo^{4+} $3d_{5/2}$ [b]			230.1

[a] Ref. [7].
[b] Ref. [8].